

DESIGN AND INTERNAL FLOW SIMULATION OF A VERTICAL HYDRAULIC TRANSPORT SYSTEM FOR MINING MANGANESE NODULES

Wijk¹, Jort M. van and Smit², Pieter M.

¹senior research engineer, jm.vanwijk@mtiholland.com, MTI Holland / Royal IHC, Smitweg 6, 2961 AW, Kinderdijk, The Netherlands, www.mtiholland.com, www.ihcmerwede.com

²research engineer, pm.smit@ihcmerwede.com, MTI Holland / Royal IHC, Smitweg 6, 2961 AW, Kinderdijk, The Netherlands, www.mtiholland.com, www.ihcmerwede.com

Abstract: On the bottom of the oceans, at depths of several kilometers, large amounts of polymetallic nodules can be found. These nodules contain high concentrations of valuable metals and thus they are a potential resource. Mining these resources requires excavation or collection and the transport of these nodules from the seafloor to the sea surface. In this paper we present the hydraulic design and the internal flow analysis of a vertical hydraulic transport system for mining manganese nodules. This system will be analysed using a one-dimensional drift-flux model, based on conservation of momentum, continuity and the advection-diffusion equation. With this model, we study the internal flow for the case of failure of a booster station.

KEY WORDS: vertical hydraulic transport, deep sea mining, flow assurance, numerical model

NOTATION

Symbol	Description	Unit
c_v	Volume fraction of solids	-
C_D	Drag coefficient	-
d	Particle diameter	m
D	Riser diameter	m
f	Wall friction coefficient	-
g	Gravitational acceleration	m/s ²
K	Number of fractions in particle size distribution	-
L	Length	m
n	Richardson and Zaki exponent	-
p	Pressure	Pa
p_e	External pressure source (e.g. pump)	Pa
P_h	Hydraulic power	W
q_s	Solids production	kg/s
SEC	Specific Energy Consumption	J/kgm
Stk	Stokes Number	-
t	time	s
v_f, v_m, v_s	Fluid, mixture and solids velocity	m/s
w_t, w_h	Terminal settling velocity, hindered settling velocity	m/s

z	vertical coordinate	m
$\varepsilon_z, \varepsilon_{Taylor}$	Axial dispersion coefficient	m^2/s
Φ	Internal friction angle	$^\circ$
ν_f, μ_f	Fluid Viscosity (kinematic, dynamic)	$m^2/s, Pa \cdot s$
μ_k	Coulomb friction coefficient	-
ρ_f, ρ_m, ρ_s	Fluid density, mixture density, solids density	kg/m^3
τ_f, τ_m, τ_s	Fluid, mixture and solids wall shear stress	Pa

1. INTRODUCTION

It was in the years 1872 – 1876 that the crew of the *H.M.S Challenger* was one of the first to discover manganese nodules on the bottom of our oceans. With just a rope and fishing net, they were able to collect some nodules from the seafloor (Murray and Renard, 1876).

Real interest in mining these deposits emerged about one hundred years later, when J.L. Mero published his book on deep sea deposits (Mero, 1965). Since then technology development in the field of deep sea mining has been progressing at varying pace. In 2012, partners from industry and academia all around Europe joined forces in the Blue Mining consortium to advance the state of the art in deep sea mining.

One of the deposits of interest to the group is manganese nodules, and one of the technological challenges under investigation is the vertical hydraulic transport of nodules from the seafloor to the sea surface. In this paper, we present a design method for the Vertical Transport System (VTS) and we use this method to design a system for transport of manganese nodules from 5000 m water depth. Furthermore, we present a one-dimensional model that we use for simulation of different transient flow scenarios.

2. VTS DESIGN METHOD

The VTS design method comprises riser internal diameter optimization, centrifugal pump size selection, nominal mixture density determination and booster station spacing optimization. The method has an iterative character.

The choice of parameters is bound to the constraint of minimum d/D ratio (which we take 1/3), the constraint of minimum bulk velocity in the riser, the constraint of minimum allowable pressures in the VTS and optimization of the Specific Energy Consumption, $EC = P_h / (L \cdot q_s)$. The power consumption is a function of the riser diameter since it determines the irreversible hydraulic losses. Moreover the centrifugal pump efficiencies together with the effect of solids on the pump performance are included in the calculation of the power consumption.

The minimum bulk velocity is defined by twice the terminal settling velocity of a spherical particle with diameter d_{90} . The drag coefficient is modelled according to Brown and Lawler (2003). Wall friction is modelled with Equations 11 and 12.

The nominal mixture density and design velocity together determine the delivered amount of solids. The density is chosen such that the minimum production requirements

are met while requiring a bulk velocity slightly larger than the minimum transport velocity, but still with the specific energy consumption as low as possible.

The VTS requires a relatively large pressure compared to the flow rate in the system, which forces the centrifugal pump to work outside the Best Efficiency Point. Choosing the suction diameter of the centrifugal pump smaller than the riser diameter improves the point of operation of the centrifugal pumps, thus increasing the overall system's efficiency. This exercise can be conducted when pump performance data is available.

Booster station spacing is important for assuring a suitable pressure operating range in the riser, while minimizing the overall weight of the riser structure itself. The minimum allowable pressure follows from the structural design of the VTS and it is prescribed by design standards. The structural design and its considerations are outside the scope of the present study.

3. 1D MODEL FOR INTERNAL FLOW SIMULATION

The mixture consists of solid particles (nodules), divided in K fractions (discrete PSD) with density $\rho_{s,k}$ suspended in seawater with density ρ_f . The total volume fraction of solids is computed as $c_v = \sum_{k=1}^K c_{v,k}$, which relates to the total mixture density as $\rho_m = \sum_{k=1}^K c_{v,k} \cdot \rho_{s,k} + (1 - \sum_{k=1}^K c_{v,k}) \cdot \rho_f$.

The 1D model consists of the conservation of mass and momentum equations for the mixture (Hiltunen et al., 2009):

$$\frac{\partial \rho_m}{\partial t} + \frac{\partial \rho_m \cdot v_m}{\partial z} = 0 \quad (1)$$

$$\begin{aligned} \frac{\partial \rho_m \cdot v_m}{\partial t} + \frac{\partial \rho_m \cdot v_m^2}{\partial t} &= \frac{\partial p}{\partial z} - \frac{4 \cdot \tau_m}{D} - \rho_m \cdot g + \sum \frac{\partial p_e}{\partial z} - \dots \\ \dots - \frac{\partial}{\partial z} &\left[(1 - c_v) \cdot \rho_f \cdot (v_m - v_f)^2 + \sum_{k=1}^K c_{v,k} \cdot \rho_{s,k} \cdot (v_m - v_{s,k})^2 \right] \end{aligned} \quad (2)$$

Equations 1 and 2 are solved by using a fractional step method. Particle transport is calculated by solving the Advection-Diffusion Equation for each fraction:

$$\frac{\partial c_{v,k}}{\partial t} + \frac{\partial c_{v,k} \cdot v_{s,k}(c_v)}{\partial z} = \frac{\partial}{\partial z} \cdot \epsilon_z \cdot \frac{\partial c_{v,k}}{\partial z} \quad (3)$$

Equation 3 is solved using the Lax-Wendroff scheme with Van Leer flux limiters. We have implemented a maximum packing limiter in the model to enforce $c_v \leq 0.6$. This limiter acts on Equation 3 by suppressing the inward fluxes to a cell when the maximum volume fraction of solids is reached.

The driving force behind the flow is the action of the centrifugal pump booster stations, modelled as $\sum \partial p_e / \partial z$ in Equation 2. Booster station dynamics are included by a limiter function along which the pressure can change. A booster station typically needs a few seconds to increase its revolutions from zero to maximum. The pressure development in time follows a quadratic curve which is used as the limiter function. The change from one pressure p_e to another always follows this limiter function. The pump

pressure is corrected for the mixture density at the position of the pump with a factor ρ_m/ρ_f . The mixture velocity inside the riser is controlled by means of a PID controller, which controls all booster stations simultaneously. The delivered pressure of a booster station thus is in the range $\langle 0, \frac{\rho_m}{\rho_f} \cdot p_{e,f} \rangle$, with $p_{e,f}$ the pressure of a booster station pumping water.

The solids transport velocity $v_{s,k}$ is modelled according to the drift flux approach, using hindered settling theory:

$$v_{s,k} = v_m + \sum_{k=1}^K c_{v,k} \cdot \frac{\rho_{s,k}}{\rho_m} \cdot w_{h,k} - w_{h,k} \quad (4)$$

The hindered settling velocity $w_{h,k}$ of an individual particle in a batch of particles is modelled with Richardson and Zaki (1954) and Mirza and Richardson (1979):

$$w_{h,k} = w_t \cdot 10^{-\frac{d}{D}} \cdot (1 - c_v)^{n-1} \quad (5)$$

The terminal settling velocity of a single, irregularly shaped particle can be modelled in several ways. We use the work of Ferguson and Church (2004):

$$w_t = \frac{\rho_s - \rho_f}{\rho_f} \cdot g \cdot d^2 \cdot \left[24 \cdot \nu_f + \left(0.75 \cdot \frac{\rho_s - \rho_f}{\rho_f} \cdot g \cdot d^3 \right)^{0.5} \right]^{-1} \quad (6)$$

The exponent n in Equation 5 is modelled according to Rowe (1987):

$$n = \frac{4.7 + 0.41 \cdot Re_p^{0.75}}{1 + 0.175 \cdot Re_p^{0.75}} \quad (7)$$

With the particle Reynolds number Re_p given by $Re_p = \rho_f w_t d / \mu_f$.

The axial dispersion term ϵ_z in Equation 3 is dependent on the Stokes number of the sediment Stk (Van Wijk et al., 2014b). Highly inert particles ($Stk \gg 1$) hardly show axial dispersion, while for $Stk \ll 1$ the model of Taylor (1954) seems a good approximation. The following is implemented:

$$\begin{aligned} \epsilon_z &= \epsilon_{Taylor} \cdot (1 - 2/3 \cdot Stk) & \text{if } Stk \leq 1.5 \\ \epsilon_z &= 0 & \text{if } Stk > 1.5 \end{aligned} \quad (8)$$

Taylor dispersion is given by:

$$\epsilon_{Taylor} = 10.1 \cdot \frac{D}{2} \cdot \frac{\sqrt{\tau_f}}{\sqrt{\rho_f}} \quad (9)$$

The Stokes number is given by:

$$Stk = \frac{4 \cdot (\rho_s - \rho_f) \cdot d \cdot v_m}{3 \cdot \rho_f \cdot D \cdot w_t \cdot C_D} \quad (10)$$

The drag coefficient C_D can be found from $w_t = \sqrt{\frac{4}{3} \cdot \frac{(\rho_s - \rho_f)}{\rho_f} \cdot \frac{g \cdot d}{C_D}}$ using Equation 6.

All viscous forces and friction are modelled with a single wall shear stress term τ_m in Equation 2. This term consists of two parts, i.e. $\tau_m = \tau_f + \tau_s$. The wall shear stress of the carrier fluid is modelled with:

$$\tau_f = \frac{f}{8} \cdot \rho_f \cdot v_f^2 \quad (11)$$

In Equation 11, f denotes the Moody friction factor for fully turbulent flow, which typically is $f \approx 0.01-0.02$ for steel risers. The solids contribution τ_s for $c_v < 0.6$ is given by Ferre and Shook (1998) :

$$\tau_s = 0.0214 \cdot \left(\frac{\rho_s \cdot v_m \cdot d}{\mu_f} \right)^{-0.36} \cdot \left(\frac{d}{D} \right)^{0.99} \cdot \left(\left[\left(\frac{c_{v,max}}{c_v} \right)^{\frac{1}{3}} - 1 \right]^{-1} \right)^{1.31} \cdot \rho_s \cdot v_m^2 \quad (12)$$

In the limit $c_v \rightarrow c_{v,max}$ Equation 12 goes to $+\infty$ with $c_{v,max} = 0.6$. In Van Wijk et al. (2014a) it has been shown however that wall friction of solid plugs is actually limited to a finite amount of friction. The model of Van Wijk et al. (2014a) is used for the case $c_v = 0.6$:

$$\tau_s = \frac{D}{4} \cdot (\rho_s - \rho_f) \cdot c_v \cdot g \cdot \left[1 - \frac{D}{4 \cdot \mu_k} \cdot \frac{1 + \sin \Phi}{1 - \sin \Phi} \cdot \frac{1}{L} \cdot \left(1 - e^{\frac{4 \cdot \mu_k}{D} \cdot \frac{1 - \sin \Phi}{1 + \sin \Phi} L} \right) \right] \quad (13)$$

4. VTS DESIGN FOR MINING POLYMETALLIC NODULES

One of the areas of interest for manganese nodule mining is the Clarion Clipperton Zone (CCZ). The seawater temperature at a depth of several kilometers is relatively constant. Data on the water temperatures in the CCZ as retrieved from the NOAA database (NOAA, 2015) indicate that the intake water temperature at 5000 m below sea level is about 5°C. The water density is $\rho_f = 1025 \text{ kg/m}^3$, the dynamic viscosity is $\mu_f = 1.7 \cdot 10^{-3} \text{ Pa s}$. The nodules have a density $\rho_s = 2500 \text{ kg/m}^3$. The design mixture density is $\rho_m = 1200 \text{ kg/m}^3$, equivalent to $c_v = 0.12$. A particle size distribution of the nodules in the CCZ is shown in Figure 1.

Given the maximum expected particle size and the required solids production, the VTS requires an internal diameter $D = 0.356 \text{ m}$. It has 12 centrifugal pumps, distributed over 6 booster stations. To meet the design velocity of $v_m = 4 \text{ m/s}$, each pump should deliver $p_{ef} = 7.4 \text{ bar}$. Including redundancy for pump failure gives $p_{ef} = 8.6 \text{ bar}$. The redundancy is based on maintaining the minimum flow rate with only five booster stations.

Roughly 83% of the required pump pressure is due to the static weight of the mixture, and about 17% is determined by friction. As a consequence, the system shows potentially

instable behavior: only a minor dip in the delivered pressure (due to a short power black-out for instance) will result in termination of production. The mixture in the VTS slows down to 0 m/s in only a few seconds. Redundancy in drive and pump capacity will be necessary for safe operation. The final VTS design is shown in Figure 2.

5. INTERNAL FLOW CALCULATIONS: SIMULATION OF PUMP FAILURE

Our transient internal flow analysis considers the simulation of the bottom booster station failure (Figure 2). After 1250 seconds of production (when the riser is just filled to the top with slurry), the bottom booster station stops working. The inflow of mixture has $c_v = 0.12$, the velocity setpoint is $v_m = 4\text{ m/s}$. Figure 3 shows the results for the cases with $p_{e,f} = 7.4\text{ bar/pump}$ and $p_{e,f} = 8.6\text{ bar/pump}$. The pressure of 7.4 bar/pump is sufficient to operate the system when all pumps are working correctly. The design value of 8.6 bar/pump includes redundancy so in case of failure the system should still be able to operate at the minimum transport velocity.

In the 8.6 bar/pump case the velocity drops to $v_m = 3.7\text{ m/s}$ which is sufficient to maintain production. In the 7.4 bar/pump case however the velocity drops to $v_m = 0.5\text{ m/s}$. The transport velocity of the largest particles is about -0.001 m/s in this case, so only the smaller particles leave the riser, shown in Figure 3c. The larger particles will settle slowly or remain suspended in the riser, which increases the risk of blockage (Van Wijk et al., 2015). Due to the low velocity, the consumed power is also small. Not the power, but the maximum attainable booster station pressure is the limiting factor.

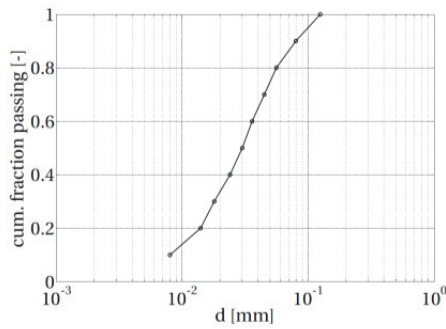


Fig. 1. Particle Size Distribution of a typical manganese nodule sample from the CCZ.

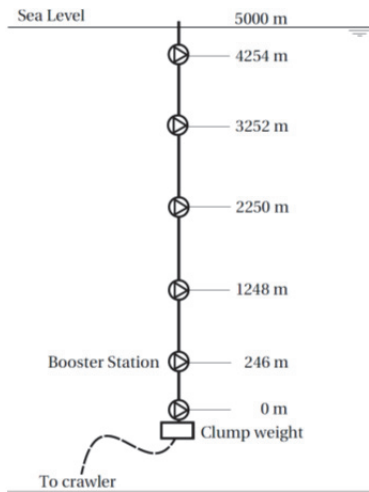


Fig. 2. Schematic layout of the vertical transport system (VTS) using the VTS coordinate system.

6. CONCLUSIONS AND RECOMMENDATIONS

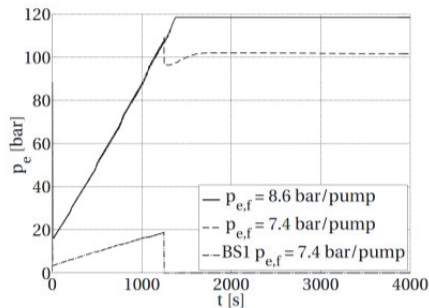
Designing the optimal VTS is an iterative exercise. Steady state analysis of the VTS gives insight in the point of operation and (specific) energy consumption, which is sufficient for the design, but transient flow analysis can be a valuable aid. The model presented in this paper is capable of transient system analysis, and therefore it can be used for the design of emergency strategies.

Due to the nature of the system (i.e. dominant static weight of the mixture), minor relative fluctuations in pump pressure can lead to large fluctuations in mixture velocity. Including pump redundancy therefor is necessary for safe operation. We have given an example of internal flow analysis for the case of pump failure. Without redundancy in pump capacity the system shows dramatic failure, while with pressure overcapacity the system still works well after failure of one booster station.

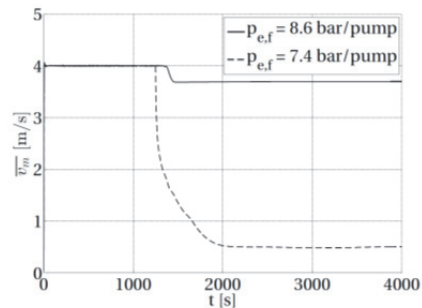
In the present model PID control is implemented for booster station control, which acts simultaneously on all pumps. The model presented in this paper can be used for development and testing of more sophisticated control strategies.

ACKNOWLEDGEMENTS

The test case presented in this paper is defined by the Blue Mining project consortium, which is supported by the European Union's Seventh Framework Program for research, technological development and demonstration under Grant Agreement no. 604500.



a. Total booster pressure and the failure of the first booster (BS1) for the 7.4 bar case and the 8.6 bar case.



b. Mixture velocity in the VTS for the 7.4 bar case and the 8.6 bar case.

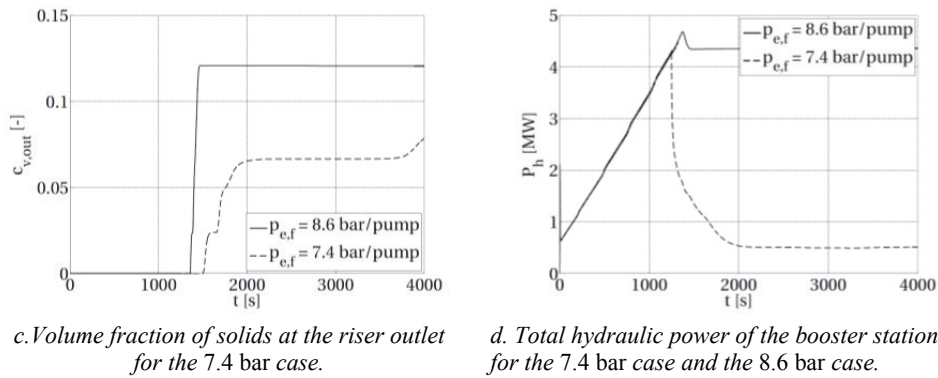


Fig.3. Results of the simulation of booster station failure.

REFERENCES

1. Brown, P.P. and Lawler, D.F. 2003. Sphere drag and settling velocity revisited. *J. Environ. Eng.* 3, 222-231.
2. Ferguson, R.I. and Church, M. 2004. A simple universal equation for grain settling velocity. *Journal of Sedimentary Research* 74, 933-937.
3. Ferre, A.L. and Shook, C.A. 1998. Coarse particle wall-friction in vertical slurry flows. *Particulate Science Technology* 16, 125-133.
4. Hiltunen, K.; Jäsberg, A.; Kallio, S.; Karema, H. Kataja, M.; Koponen, A.; Manninen, M. and Taivassalo, V. 2009. Multiphase flow dynamics. VTT Publications 722, Helsinki.
5. Murray, J. and Renard, A.F. 1876. Report on deep-sea deposits based on the specimens collected during the voyage of the H.M.S. Challenger in the years 1872-1876. The H.M.S. Challenger Library, <http://19thcenturyscience.org/HMSC>.
6. Mero, J.L. 1965. The mineral resources of the sea. Elsevier Oceanography Series vol. 1. Elsevier, Amsterdam.
7. Mirza, S. and Richardson, J.F. 1979. Sedimentation of particles of two or more sizes. *Chem. Eng. Sc.* 34.
8. National Oceanographic and Atmospheric Administration. National oceanographic data center world ocean database. <http://www.nodc.noaa.gov>. Data retrieved in January 2015.
9. Richardson, J.F. and Zaki, W.N. 1954. Sedimentation and fluidization part I. *Trans. Instn. Chem. Engrs.* 32.
10. Rowe, P.N. 1987. A convenient empirical equation for estimation of the Richardson and Zaki exponent. *Chem. Eng. Sc.* 42.
11. Taylor, G.I. 1954. The dispersion of matter in turbulent flow through a pipe. *Proc. Royal Society A.* 223.
12. Wijk, J.M. van; Rhee, C. van and Talmon, A.M. 2014. Wall friction of coarse grained sediment plugs transported in a water flow through a vertical pipe. *Ocean Engineering* 79, 50-57.
13. Wijk, J.M. van; Rhee, C. van and Talmon, A.M. 2014. Axial dispersion of suspended sediments in vertical upward pipe flow. *Ocean Engineering* 94, 20-30.
14. Wijk, J.M. van; Grunsven, F. van; Talmon, A.M. and Rhee, C. van. 2015. Simulation and experimental proof of plug formation and riser blockage during vertical hydraulic transport. *Ocean Engineering* 101, 58-66.